1975LPSC....6..987T

Proc. Lunar Sci. Conf. 6th (1975), p. 987–996.
Printed in the United States of America

Relative cooling rates of mare basalts at the Apollo 12 and 15 sites as estimated from pyroxene exsolution data

HIROSHI TAKEDA and MASAMICHI MIYAMOTO

Mineralogical Institute, Faculty of Science, University of Tokyo,
Hongo, Tokyo 113, Japan

TERUAKI ISHII

Geological Institute, Faculty of Science, University of Tokyo,
Hongo, Tokyo 113, Japan

GARY E. LOFGREN

NASA Johnson Space Center, Houston, Texas 77058

Abstract—X-ray single-crystal diffraction studies, supplemented by electron microprobe analyses of core pigeonites and rim augites from rocks 12031, 15085, 15475, and 15495, have been used to suggest cooling rates for these and other Apollo 12 and 15 rocks studied by similar methods. The extent of subsolidus phase separation of pyroxenes is used as a measure of the cooling rate. The results were interpreted in terms of model cooling histories of a lava flow whose thickness was estimated from the absolute cooling rates obtained by cooling rate experiments and by temperature–time variation through an extrusive flow computed by employing simplified theory of Jaeger. All available data on the exsolution and cation distributions of pyroxenes from Apollo 12 and 15 samples at present are consistent with the hypothesis that these rocks were derived from the top and interior of lava flows with thicknesses of 4–10 m. A process for exsolution of augite from a host pigeonite on (100) has been related to its low-calcium content.

INTRODUCTION

RECENT PUBLISHED REPORTS on the exsolution of various pyroxenes in quartz-normative (QN) basalts from diverse localities at the Apollo 12 and 15 sites (e.g. Papike *et al.*, 1971, 1972) are difficult to correlate with cooling rates appropriate for various depths within a mare lava flow. More comprehensive, comparative studies on pyroxene exsolution and cooling rates of mare basalts may help to improve our understanding of the cooling history of mare lava flows. Exsolution data on pyroxenes from slowly cooled rocks are particularly important because such data determine the maximum thickness of a flow. Pyroxenes from QN basalts, 12031,10, 15085,66, 15475,58, and 15495,112, have been studied by single-crystal X-ray diffraction and microprobe techniques for such purpose. Slow cooling histories are suggested for these rocks. The results, combined with other available data on pyroxenes from QN basalts, are ranked according to subsolidus cooling rate.

Lofgren *et al.* (1974, 1975) and Taylor *et al.* (1975) estimated absolute cooling rates of some of the QN basalts from their cooling rate experiments. In order to compare these results with those of pyroxene exsolution data, temperature–time

© Lunar and Planetary Institute • Provided by the NASA Astrophysics Data System

1975LPSC....6..987T

variations through an extrusive flow with assumption that upper surface is at zero temperature, have been computed using the simplified theory given by Jaeger (1968). In this paper we compare the extent of pyroxene exsolution to the cooling rate experiments and the calculated cooling rates and then estimate thickness of the mare basalt flow that contained them. The results provide one test of the hypothesis that the rocks could have come from various depths of one lava flow.

Experimental Studies and Results

Approximately thirty crystals were separated under a microscope from three rock chips 15085,66, 15475,58, and 15495,112 and from a pyroxene concentrate 12031,10. Exsolution lamellae were not visible by light optics. Crystal fragments 0.1–0.3 mm in average dimension were mounted with c^* parallel to a glass fiber, and precession photographs of the $h0l$ and $0kl$ nets were taken using Zr-filtered, Mo Kα radiation. The cell dimensions, the relative orientation, and the space-group symmetry of the host and exsolved pyroxenes are given in Table 1. These crystals were subsequently analyzed by microprobe techniques (Table 2). In some cases, a crystal measuring approximately 0.5 mm in length was broken in half, and one fragment was used for the X-ray study and the other for microprobe analysis.

Rock 12031 has coarse grained holo-crystalline texture, but the sample we studied is a pyroxene concentrate 12031,10. The maximum length of the crystals is about 0.2 mm. Microprobe analyses of about ten grains indicate that Fe-rich augites are dominant and that the chemical zoning trend is similar to that of 12021 (Ross *et al.*, 1973). X-ray precession photographs of a 12031 subcalcic ferroaugite show exsolved pigeonite oriented on (001). Amount of exsolved pigeonite is almost equal to that of the host augite, according to volume estimates made by visual comparison of the diffracted intensities of each phase. The mean $\Delta\beta = \beta(\text{pig.}) - \beta(\text{aug.})$ for the 12031 pyroxene is 2.84° (Table 1).

Table 1. Crystallographic data on pyroxenes from rocks 12031, 15495, 15475, and 15085.

Sample number	Crystal number	Pyroxenes	a (Å)	b (Å)	c (Å)	β(°)	Space group
12031	A1	Augite	9.76	9.00	5.258	105.83	$C2/c$
		(001) Pigeonite	9.76	9.00	5.247	108.67	$P2_1/c$
15495	P5	Pigeonite	9.66	8.88	5.21	108.5	$P2_1/c$
15495	P14	Pigeonite	9.67	8.89	5.22	108.5	$P2_1/c$
		(001) Augite	9.67	8.89	5.26	106.3	$C2/c$
15495	A10	Augite	9.71	8.92	5.26	106.6	$C2/c$
		(001) Pigeonite	9.71	8.92	5.22	108.7	$P2_1/c$
15475	A2	Augite	9.74	8.95	5.253	105.98	$C2/c$
		(001) Pigeonite	9.74	8.95	5.232	108.85	$P2_1/c$
15085	P1	Pigeonite	9.68	8.90	5.212	108.67	$P2_1/c$
		(001) Augite	9.68	8.90	5.258	106.10	$C2/c$

Cell dimensions have estimated errors of ±0.2%.

© Lunar and Planetary Institute • Provided by the NASA Astrophysics Data System

1975LPSC....6..987T

Rock 15495 is coarse grained and contains euhedral pyroxene prisms up to 25 × 3 mm with a pigeonite core and thin augite rims, similar in size to those in rock 12021 which had a relatively slow subsolidus cooling history (Papike *et al.*, 1971). Single crystals of core pigeonite (P4, P5) and rim augite (A10) were separated from one phenocryst (3 × 1.5 mm) attached to a small rock fragment 15495,112 (weight 0.103 g).

The core pigeonites show virtually no exsolved augite, but very faint diffuse spots of augite with common a^* direction that originate from pigeonite reflections parallel to the a^* have been observed on one $h0l$ photograph after exposures of 68 hr. This (100) augite has a β^* angle 1.3° larger than that of the pigeonite. The "b" reflections ($h + k$ odd) are slightly diffuse indicating moderate domain size. The composition of the core pigeonite, $Ca_{5.9}Mg_{67.5}Fe_{26.6}$; is similar to those of the core centers of 12065 (Kushiro *et al.*, 1971) and 15476 (Kushiro, 1973) which are low-calcium pigeonites, but have a higher calcium content than the 15495 pigeonite. In spite of the low-calcium content of this pyroxene which is close to that of the so-called hypersthene core of the 12065 pyroxene reported by Hollister *et al.* (1971), no orthopyroxene reflections were observed on the X-ray photographs. The chemical trends of the 15495 pyroxenes are similar to that of 15476.

X-ray precession photographs of a calcium-rich portion (P2) $Ca_{9.1}Mg_{60.6}Fe_{30.2}$ of the above core pigeonite and a high-calcium pigeonite grain (P14) $Ca_{9.2}Mg_{61.0}Fe_{29.8}$ in rock 15495, show weak reflections of exsolved augite oriented on (001), in addition to the diffuse (100) augite reflections exhibited by crystal P5. The photographs of the rim augite $Ca_{33.2}Mg_{42.7}Fe_{24.1}$ (A10) indicate that they contain exsolved pigeonite in (001) orientation, and that a small fragment of core pigeonite sharing approximately (100) plane were left on the augite because of incomplete separation. The angle between the a^* direction of the core and exsolved

Table 2. Representative electron microprobe analyses of pyroxenes (wt.%) from rocks 12031, 15495, 15475, 15085, and 14310.

Sample	12031,10	15495,112				15475,58			15085,66		14310,413
Crystal	A1	P5	P2	P14	A10	P1	P4	A2	A1	P1	R75
SiO_2	47.9	52.5	52.2	52.0	49.2	53.0	53.1	48.3	50.3	52.6	52.2
Al_2O_3	0.96	1.25	1.35	1.42	3.79	0.95	1.07	2.03	2.91	1.24	1.75
TiO_2	1.15	0.31	0.34	0.37	0.99	0.27	0.26	1.36	0.85	0.32	0.57
Cr_2O_3	0.21	0.93	0.92	0.91	1.22	0.95	0.83	0.45	0.91	0.70	0.43
FeO	29.5	17.1	19.0	18.8	14.4	17.0	18.0	23.7	12.6	19.4	17.8
MnO	0.46	0.31	0.36	0.35	0.26	0.29	0.36	0.35	0.18	0.36	—
MgO	7.98	24.3	21.4	21.6	14.3	24.8	23.4	10.3	14.5	20.8	23.8
CaO	11.3	2.95	4.49	4.54	15.5	2.66	3.05	13.1	17.4	4.68	2.35
Na_2O	0.02	0.05	0.04	0.00	0.06	0.00	0.02	0.02	0.04	0.00	—
Total	99.5	99.7	100.1	100.0	99.7	100.0	100.1	99.7	99.7	100.1	98.9
Ca*	24.9	5.9	9.1	9.2	33.2	5.3	6.1	28.5	36.7	9.6	4.8
Mg	24.4	67.5	60.6	61.0	42.7	68.4	65.6	31.2	42.6	59.3	67.1
Fe	50.7	26.6	30.2	29.8	24.1	26.3	28.3	40.3	20.7	31.1	28.1

*Atomic %.

© Lunar and Planetary Institute • Provided by the NASA Astrophysics Data System

1975LPSC....6..987T

pigeonites is 0.81°. The mean $\Delta\beta$ for the 15495 pyroxene crystals studied is 2.2° (Table 1).

Cation distribution of the low-calcium pigeonite (P4), has been determined by least-squares techniques using X-ray intensities measured with a single-crystal diffractometer. The weighted *R*-value is 0.025 for 1424 reflections. Site populations and mean M–O bond distances of a preliminary refinement; M1 (0.904Mg + 0.073Fe + 0.023Cr,Ti), 2.085 Å; M2 (0.415Mg + 0.462Fe + 0.123Ca), 2.213 Å, indicate considerable ordering. The cation distribution coefficient, $k = (Fe/Mg)_{M1}/(Fe/Mg)_{M2}$ of the 15495 pigeonite is 0.072.

Rock 15475 is a pigeonite porphyry similar to rock 15476 described by Kushiro (1973). Single crystals of core pigeonite and rim augite were separated from one phenocryst (3 × 2 mm) in rock fragment 15475,58. A low-calcium pigeonite core $Ca_{6.1}Mg_{65.6}Fe_{28.3}$ (P4), moderate yellow green, is surrounded by augite rims $Ca_{28.5}Mg_{31.2}Fe_{40.3}$ (A2). The compositional trend from low-calcium pigeonite (P1) $Ca_{5.3}Mg_{68.4}Fe_{26.3}$ to iron-rich subcalcic augite $Ca_{24.2}Mg_{21.8}Fe_{53.9}$, is also similar to that of 15476. Pigeonite crystals (P1, P4) in rock 15475 show faint short diffuse streaking that originates from pigeonite reflections and is parallel to approximately [101]* direction. The rim augite (A2) has exsolved about 40% of pigeonite. The $\Delta\beta$ angle for this pair is 2.87° (Table 1).

Rock 15085 has an intergranular texture and the plagioclase is nearly as large as the pyroxene. Lofgren *et al.* (1975) suggested that this rock to be one of the most slowly cooled rocks among the Apollo 15 QN basalts. Single crystals for the X-ray work were separated from a pyroxene phenocryst (4.5 × 2 mm) in one of rock chips 15085,66 (weight 0.155 g). The compositional trend is from low-calcium core pigeonite $Ca_{5.4}Mg_{67.5}Fe_{27.1}$ to $Ca_{9.6}Mg_{59.3}Fe_{31.1}$ (P1), and to rim augite (A1) $Ca_{36.7}Mg_{42.6}Fe_{20.7}$. These pigeonites from 15085 contain augite oriented on both (001) and (100); however, the lack of distinct core–rim relationships between two pyroxenes, makes it difficult to separate epitaxial and exsolution relations. A subcalcic augite exsolves pigeonite on (001), and $\Delta\beta$ for this pair is 2.4°.

Calculation of Temperature–Time Variations of a Model Mare-Lava Flow

Simplified theories to calculate temperatures in various cooling igneous bodies have been treated by Jaeger (1968). Considering extremely high rates of lava extrusion with low viscosity of the basalt melt and photographic observations of the mare-lava flows (Schaber, 1973), we have chosen a formula given for an extrusive flow with the upper surface at zero temperature as suitable for lunar mare-lava flow. The temperature T at time t at distance x from the mid-plane of the sheet of thickness $2a$ is given by

$$T/T_0 = \phi(\xi, \tau) - \phi(2 - \xi, \tau),$$

$\phi(\xi, \tau)$ is expressed by the difference of two error functions (Jaeger, 1968), where $\xi = x/a$ and $\tau = \kappa t/a^2$, and T_0 is initial temperature of magma and κ is thermal diffusivity.

© Lunar and Planetary Institute • Provided by the NASA Astrophysics Data System

1975LPSC....6..987T

Temperature–time variations through an extrusive sheet of thickness $2a$ (a = 1, 2, 3, 5, 6, 10, and 15 m) have been computed assuming thermal diffusivity $\kappa = 0.004\ cm^2/sec$ (Horai and Winkler, 1974). Figure 1 is an example for a = 3 m. The computation represents a first approximation, and for more detailed studies convection, release of latent heat of crystallization, the temperature dependence of κ, the effect of presence of gases, etc., should be taken into account.

Discussion

The Apollo 15 phenocrysts studied in this paper are characterized by chemically homogeneous cores of low-calcium pigeonite. The cores typically occupy about three-quarters of the phenocrysts, but their extent varies from grain to grain. For convenience, we divide pigeonites into two groups: low-calcium pigeonite with a calcium content less than that of pigeonite at its lowest stability field (*ca.* 8 atom% of Ca; Yang, 1973; Ross *et al.*, 1975) and high-calcium pigeonite with a greater calcium content than the limit given above. In 15495, pigeonites that exsolved augite oriented on (001) were all of the high-calcium variety. Low-calcium pigeonites exhibited diffuse augite reflections suggesting fine scale lamellae on (100). The presence of low-calcium pigeonite, $Ca_{4.8}Mg_{67.7}Fe_{28.1}$, was also confirmed for a pigeonite crystal of 14310,413 R75 (Table 2) which exhibits both (001) and (100) augite reflections (Takeda and Ridley, 1972). Virgo and Ross (1973) reported pigeonite, $Ca_{4.0}Mg_{40.5}Fe_{55.4}$, with (100) augite from the Mull andesite, and in 12021 Ross *et al.* (1973) observed that calcium-poor pigeonite exsolved augite oriented on (100) and (001) while calcium-rich pigeonite exsolved augite only on (001). Since such low-calcium pigeonite, which crystallized on the pigeonite solidus, may not unmix augite until it reaches the metastable extension of the pigeonite solvus (Huebner *et al.*, 1975; Ishii and Takeda, 1974), investigation of the genesis of the (100) augite exsolution should take into account the exsolution process.

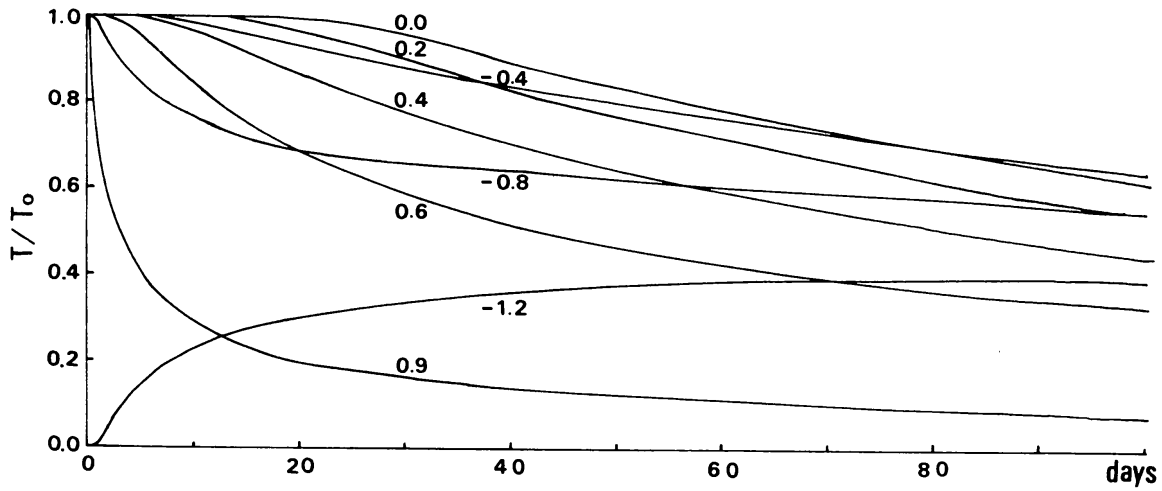

Fig. 1. Temperature–time variations at various depths of an extrusive flow of thickness $2a$ = 6 m. Numbers on the curves are values of $\xi = x/a$. x: position coordinates, ξ = 1.0 at the surface, ξ = 0.0 at the center, negative ξ = below center of flow. T_0: initial temperature of magma, 1200°C was assumed.

© Lunar and Planetary Institute • Provided by the NASA Astrophysics Data System

1975LPSC....6..987T

The low-calcium content of the core pigeonites may not be adequate for ranking relative cooling rates of the mare rocks, because the lack of augite exsolution in the pigeonite depends not only on rapid cooling, but also on the total calcium content—i.e. on the lack of suitable nucleation sites.

The $\Delta\beta = \beta(\text{pig.}) - \beta(\text{aug.})$ of pigeonite–augite pairs sharing common (001) in subcalcic augites and high-calcium pigeonites has been used to estimate the degree of phase separation. Although the $\Delta\beta$ angle has been used as a measure of subsolidus cooling history by many investigators (Papike *et al.*, 1971; Ghose *et al.*, 1972), one should not ignore the fact that different exsolution mechanisms will produce different "extent of exsolution" for similar cooling rates and similar "extent of exsolution" for dissimilar cooling rates. For instance, if pigeonite exsolved augite by nucleation and growth, the augite precipitate would have the equilibrium composition. On the other hand, if the pigeonite exsolved augite by spinodal decomposition, the precipitate will have a range of compositions; and only after coarsening will it reach the compositional state (similar $\Delta\beta$) of the precipitate formed by nucleation and growth (Nord *et al.*, 1975). $\Delta\beta$ may also depend on other factors, including solidus temperature and chemical composition.

It is generally accepted that the thickness of augite lamellae is an accurate indicator of cooling rate. The thicknesses of augite lamellae observed by dark-field transmission electron micrograph (Ghose *et al.*, 1972) and their $\Delta\beta$'s suggest that the thickness increases with increasing $\Delta\beta$. Since all QN basalts we will discuss in this paper have similar chemical compositions and crystallization trends, and since the differences in rock textures are found to be related to the cooling rates, $\Delta\beta$ may be used as an indicator of subsolidus cooling rate, at least for a first approximation.

The results tabulated in Table 3, including those reported previously, may represent the approximate relative subsolidus cooling rates of Apollo 12 and 15 mare basalts between approximately 1020°C and 800°C (Ross *et al.*, 1973), the temperatures between which the exsolution is considered to develop. The sequence is somewhat different from those obtained from the phenocryst shapes and matrix textures (Lofgren *et al.*, 1975) and the kinetics of Zr partitioning between coexisting ilmenite and ulvöspinel (Taylor *et al.*, 1975). However, the phenomena used to estimate the cooling rates represent events which took place in different temperature ranges and may indicate a variation in cooling rate with temperature.

The absolute cooling rates given by the above workers can be correlated with the computed temperature–time variations at various depths of a lava flow to estimate the thickness of the flow. Once the most reliable thickness is estimated, we may be able to estimate the absolute cooling rates for a temperature range where the pyroxene exsolution took place. These data in turn will be used to explain the discrepancy of cooling-rate ranks estimated from different data.

The assumptions set for estimation of the thickness of a lava flow are: (1) the excavated rocks of the Apollo 12 and 15 samples are random samples of at least one flow, (2) the temperature–time variation curve at near $\xi = 0.0$ should satisfy the slowest cooling rate reported, 0.17°C/hr = 4°C/day (Taylor *et al.*, 1975). The

© Lunar and Planetary Institute • Provided by the NASA Astrophysics Data System

1975LPSC....6..987T

ranked* according to cooling rates on the basis of the pyroxene exsolutions. The ranges of $\Delta\beta = \beta(\text{pig.}) - \beta(\text{aug.})$ with their mean values in parentheses are given.

Apollo 15		Apollo 12	
Sample	$\Delta\beta$	Sample	$\Delta\beta$
15597[a]	1.5	—	—
15016[b]	1.5	—	—
15499[b]	1.3 (1.6) 1.8	12052[e,g]	1.58
15065[c]	1.5 (1.8) 2.2	12053[f]	1.58
15555[b]	2.1 (2.2) 2.5	12038[f]	2.25
15495[d]	2.2	12040[f]	2.25
15085[d]	2.4	12037[g]	2.5 (2.6) 2.7
15058[b]	2.5 (2.7) 2.9	12031[d]	2.84
15475[d]	2.87	12021[g]	2.4 (2.7) 3.0

[a]Brown and Wechsler (1973).
[b]Papike *et al.* (1971).
[c]Yazima and Hafner (1974).
[d]This study.
[e]Takeda (1972).
[f]Ghose *et al.* (1972).
[g]Papike *et al.* (1972).
*Slower cooling placed last in list.

relative trends of cooling histories may not depend on the thickness, because the parameters used in computation are position ratios ($\xi = x/a$), not absolute depth. Assumption (1) implies that number of samples from the interior of a flow, namely, slowly cooled ones may be larger than those from the near surface.

Most of the Apollo 15 QN rocks cooled slower than 1°C/hr (say 0.5°C/hr) (Lofgren *et al.*, 1975), thus $2a = 4$ m is a reasonable lower limit of thickness. By comparison, $2a = 30$ m is too thick because it gives cooling rate 0.005°C/hr between 1200°C and 1020°C and this is inconsistent with the large number of samples which cooled at 5–20°C/hr. It is possible that $2a = 10$ m, which gives 0.05°C/hr, may represent the maximum thickness.

Figure 1 is an example for $2a = 6$ m, for which initial cooling rate ranging from 12 to 0.16°C/hr, can be attained for various depths of the flow. These rates have been shown to reproduce the texture of Apollo 15 QN basalts (Lofgren *et al.*, 1974), and account for the abundance of samples among three groups of cooling rates (Lofgren *et al.*, 1975), which are 5–20°C/hr, 2–5°C/hr and <1°C/hr.

A thickness of 6 m is consistent with the thickness of the 2–20 m thick outcrops exposed in Hadley Rille (Howard *et al.*, 1972), but are thinner than flow thicknesses (10–63 m) estimated from photogrammetric measurements in mare Imbrium (Schaber, 1973). However, Brett (1974) reported thicknesses estimated for mare basalt flows that are all less than 5 m.

© Lunar and Planetary Institute • Provided by the NASA Astrophysics Data System

1975LPSC....6..987T

Some difficulties encountered in placing the QN basalts into Fig. 1, are due to the reverse ranking of some rock cooling rates estimated by different investigators. For example, 15065 and 15085 were ranked as the most slowly cooled rocks by Lofgren *et al.* (1975) and Taylor *et al.* (1975), while exsolution data indicate 15475 and 15058 to be the slowest cooled rocks. Taylor *et al.* (1973) reported that 15475 cooled slower than 15495 in agreement with our data.

One possible explanation for this discrepancy will be given by comparison of the curve for $\xi = 0.2$ with that for -0.4 in Fig. 1. Note that the two curves intersect at about 35 days after extrusion. By assuming that curve 0.2 represents the cooling rate of rock 15085 or 15065 and curve -0.4 that of rock 15475, we can see that 15085 had a slow initial cooling during crystallization of the lava, followed by slightly faster cooling in the temperature range where the exsolution develops, while 15475 had faster cooling rate in the beginning, and slower cooling rate during the exsolution stage. Another explanation may be that the exsolution mechanisms were different resulting in different $\Delta\beta$'s for a similar cooling rate, but the above two cooling paths are certainly possible ones.

The mean $\Delta\beta$ for the 15495 pyroxene is 2.2° which is lower than pyroxenes from rocks with smaller pyroxene phenocrysts such as 15058, for which a slow subsolidus cooling history is suggested (Papike *et al.*, 1972). If $\Delta\beta$ is a valid measure of subsolidus cooling history, the above results would indicate that rock 15495 with coarser pyroxenes may have been cooled faster than rock with medium-grain pyroxenes.

This apparent discrepancy may be explained by our simulation studies on the cooling history of a model mare-lava flow (Fig. 1). The data of Lofgren *et al.* (1974) show that phenocryst grain size may not be simply related to cooling rates. By combination of appropriately fast growth rate and slow nucleation rate of pyroxenes, large phenocrysts may grow at a particular depth of a flow. Furthermore, in some flows, as will be shown by calculation of the settling velocity of a spherical particle of density 3.45 g/cm^3 in a lava of viscosity 10 poise and density 3.10 g/cm^3, crystal settling may concentrate coarse phenocryst toward the bottom of the flow, where the cooling rate may be higher than the center (compare curves for $\xi = 0.0$ and -0.8 in Fig. 1). Thus, we cannot exclude the possibility that coarse-grain phenocrysts may show a small degree of exsolution. This is in fact the case for 15495. Therefore the $\Delta\beta$ method may be a more reliable measure of the subsolidus cooling rate, for a particular portion of the cooling history.

The curve, for example, for $\xi = 0.6$ or -0.8 compared with that of $\xi = 0.0$ or 0.2 suggests that rocks which cooled faster at high temperature (above 800°C) where exsolution develops, could show a high degree of Fe^{2+}–Mg ordering over the M1 and M2 sites in pyroxenes as were shown by the 15476 (Ohashi and Finger, 1974) and 15495 pigeonites. The cooling rates between 700°C and 500°C may eventually become similar to each other (0.3–0.2°C/hr) about 40 days after the extrusion, consequently pyroxenes showing a large variation in the degree of exsolution may show a similar degree of cation ordering (Takeda, 1972). Assuming the initial crystallization temperature of a magma as 1200°C, we estimate that the cooling rates between 1020°C and 800°C, a range within which exsolution textures may be

© Lunar and Planetary Institute • Provided by the NASA Astrophysics Data System

1975LPSC....6..987T

best developed, to be from 1.5 to 0.2°C/hr for $2a = 6$ m. Then, comparison of curves for example, for $\xi = 0.6$ and -0.8 suggest that pyroxenes with minor exsolution but with considerable Mg–Fe ordering may have cooled near the bottom of the flow, and those with similar exsolution but with disordered Mg–Fe distribution may have cooled near surface of the flow.

The model computation indicates that all available data on the exsolution and cation distributions of pyroxenes at the Apollo 12 and 15 sites up to date are consistent with hypothesis that these rocks were derived from the top and interior of lava flows with thicknesses on the order of 4–10 m. Presence of a very small number of pyroxene vitrophyres at the Apollo 12 site and absence of the 12021-type pyroxene at the Apollo 15 site suggest that rapidly cooled rocks may be more abundant at the Apollo 15 site compared to the Apollo 12 site.

In summary, (1) the degree of subsolidus phase separation of pyroxenes from quartz-normative basalts, 12031, 15085, 15475, and 15495, has been studied by single-crystal X-ray diffraction and microprobe techniques, and the relative cooling rates of these rocks and others studied by similar methods have been ranked according to the pyroxene exsolution data; (2) by combining temperature–time variation through an extrusive flow computed by employing Jaeger's theory and absolute cooling rates of the above rocks estimated by other methods, the thickness of a mare-lava flow was estimated to be from 4 to 10 m; (3) typical paths of exsolution and Mg–Fe^{2+} cation ordering at various depths of a lava flow were investigated by employing the absolute cooling rates obtained by the model computation of cooling history; and (4) a process of exsolution of augite oriented on (100) of the host low-calcium pigeonite has been proposed.

Acknowledgments—We are indebted to Prof. I. Kushiro, Dr. D. S. Mckay, and Mr. Y. Ikeda for discussion; to Profs. R. Sadanaga and Y. Takéuchi for their interest given us during this research; and to Drs. M. Ross, J. S. Huebner, and R. H. McCallister for critical reading of the manuscript. The computation and microprobe analyses were made at the University of Tokyo. We thank Mrs. M. Hatano, Misses A. Kawahara, and M. Sato for their technical assistance. Part of the work was carried out at the NASA–JSC, where one of the authors (HT) was a visiting scientist of the Lunar Science Institute in 1974 under NASA contract NSR-09-051-001. This paper constitutes Lunar Science Institute Contribution No. 223.

References

Brett R. (1974) Thicknesses of some lunar mare basalt flows and ejecta blankets based on chemical kinetic data. *Meteoritics* **9**, p. 319–320.

Brown G. E. and Wechsler B. A. (1973) Crystallography of pigeonites from basaltic vitrophyre 15597. *Proc. Lunar Sci. Conf. 4th*, p. 887–900.

Ghose S., Ng G., and Walter L. (1972) Clinopyroxenes from Apollo 12 and 14: Exsolution, domain structure, and cation order. *Proc. Lunar Sci. Conf. 3rd*, p. 507–531.

Hollister L. S., Trzcienski, Jr., W. E., Hargraves R. B., and Kulick C. G. (1971) Petrogenetic significance of pyroxenes in two Apollo 12 samples. *Proc. Lunar Sci. Conf. 2nd*, p. 529–557.

Horai K. and Winkler J. (1974) Thermal diffusivity of lunar rock sample 12002,85 (abstract). In *Lunar Science V*, p. 354–356. The Lunar Science Institute, Houston.

Howard K. A., Head J. W., and Swann G. A. (1972) Geology of Hadley Rille. *Proc. Lunar Sci. Conf. 3rd*, p. 1–14.

© Lunar and Planetary Institute • Provided by the NASA Astrophysics Data System

1975LPSC....6..987T

Huebner J. S., Ross M., and Hickling N. L. (1975) Cooling history and significance of exsolved pyroxene in lunar noritic breccia 77215 (abstract). In *Lunar Science VI*, p. 408–410. The Lunar Science Institute, Houston.

Ishii T. and Takeda H. (1974) Inversion, decomposition and exsolution phenomena of terrestrial and extraterrestrial pigeonites. *Memoir Geol. Soc. Japan* **11**, 19–36.

Jaeger J. C. (1968) Cooling and solidification of igneous rocks. In *Basalts: The Poldervaart Treatise on Rocks of Basaltic Composition* (editors H. H. Hess and A. Poldervaart), Vol. 2, p. 503–537. Wiley-Interscience, New York.

Kushiro I. (1973) Crystallization of pyroxenes in Apollo 15 mare basalts. *Carnegie Inst. Wash., Yearb.*, **72**, 647–650.

Kushiro I., Nakamura Y., Kitayama K., and Akimoto S. (1971) Petrology of some Apollo 12 crystalline rocks. *Proc. Lunar Sci. Conf. 2nd*, p. 481–495.

Lofgren G. E., Donaldson C. H., Williams R. J., Mullins O., Jr., and Usselman T. M. (1974) Experimentally reproduced textures and mineral chemistry of Apollo 15 quartz normative basalts. *Proc. Lunar Sci. Conf. 5th*, p. 549–567.

Lofgren G. E., Usselman T. M., and Donaldson C. H. (1975) Cooling history of Apollo 15 quartz normative basalts determined from cooling rate experiments (abstract). In *Lunar Science VI*, p. 515–517. The Lunar Science Institute, Houston.

Nord G. L., Jr., Heuer A. H., Lally J. S., and Christie J. M. (1975) Substructures in lunar clinopyroxenes as petrologic indicators (abstract). In *Lunar Science VI*, p. 601–603. The Lunar Science Institute, Houston.

Ohashi Y. and Finger L. W. (1974) A lunar pigeonite: Crystal structure of primitive-cell domains. *Carnegie Inst. Wash., Yearb.*, 525–531.

Papike J. J., Bence A. E., Prewitt C. T., and Wu C. H. (1971) Apollo 12 clinopyroxenes: Exsolution and epitaxy. *Earth Planet. Sci. Lett.* **10**, 307–315.

Papike J. J., Bence A. E., and Ward M. A. (1972) Subsolidus relations of pyroxenes from Apollo 15 basalts. In *The Apollo 15 Lunar Samples* (editors J. Chamberlain and C. Watkins), p. 144–147. The Lunar Science Institute, Houston.

Ross M., Huebner J. S., and Dowty E. (1973) Delineation of the one atmosphere augite–pigeonite miscibility gap for pyroxenes from lunar basalt 12021. *Amer. Mineral.* **58**, 619–635.

Schaber G. G. (1973) Lava flows in Mare Imbrium: Geologic evaluation from Apollo orbital photography. *Proc. Lunar Sci. Conf. 4th*, p. 73–92.

Takeda H. (1972) Structural studies of rim augite and core pigeonite from lunar rock 12052. *Earth Planet. Sci. Lett.* **15**, 65–71.

Takeda H. and Ridley W. I. (1972) Crystallography and chemical trends of orthopyroxene–pigeonite from rock 14310 and coarse fine 12033. *Proc. Lunar Sci. Conf. 3rd*, p. 423–430.

Taylor L. A., McCallister R. H., and Sardi O. (1973) Cooling histories of lunar rocks based on opaque mineral geothermometers. *Proc. Lunar Sci. Conf. 4th*, p. 819–828.

Taylor L. A., Uhlmann D. R., Hopper R. W., and Misra K. C. (1975) Absolute cooling rate of lunar rocks based on the kinetics of Zr diffusion in opaque oxides: Application to Apollo 15 rocks from elbow crater (abstract). In *Lunar Science VI*, p. 798–800. The Lunar Science Institute, Houston.

Virgo D. and Ross M. (1973) Pyroxenes from Mull andesites. *Carnegie Inst. Wash., Yearb.*, **72**, 535–540.

Yang H. Y. (1973) Crystallization of iron-free pigeonite in the system anorthite–diopside–enstatite–silica at atmospheric pressure. *Amer. J. Sci.* **273**, 488–497.

Yazima T. and Hafner S. S. (1974) Cation distribution and equilibrium temperature of pigeonite from basalt 15065. *Proc. Lunar Sci. Conf. 5th*, p. 769–784.

© Lunar and Planetary Institute • Provided by the NASA Astrophysics Data System